

Fluid-solid interaction analysis of torque converters^①

Zhang Zeyu(张泽宇)^②, Hui Jizhuang^②, Suo Xuefeng, Zhang Fuqiang, Lei Jingyuan

(National Engineering Laboratory for Highway Maintenance Equipment, Chang'an University, Xi'an 710064, P. R. China)

Abstract

In order to extend the service life of torque converters, it is essential to predict the pressure condition and improve its weak areas. According to computational fluid dynamics and structural statics, a model of torque converter is constructed using software ANSYS. Then, a fluid-solid interaction (FSI) analysis method is proposed to obtain its stress distribution, in which the fluid pressure is applied to the coupling surface to calculate the interaction between fluid and solid. The results show that the fluid pressure at the inlet of the impeller is maximum and decreases along the flow direction, the pressure at the inlet of the turbine blade is minimum and the outlet pressure is the largest, increasing along the flow direction gradually; the pressure distribution of the impeller is concentrated mainly at the corner, especially between the inner ring and the impeller blades; the pressure of the turbine is concentrated mainly on the connection between turbine and the outer edge of the blade.

Key words: torque converter, fluid-solid interaction (FSI), stress distribution, pressure analysis, simulation

0 Introduction

There is a fluid-solid interaction (FSI) effect between oil and blades when the torque converter is at work. On one hand, the blade can deform, break or fall under the condition of high temperature, high load, etc. On the other hand, the deformation or failure of the blade can affect the distribution of the flow field, reducing its performance and service life^[1-6].

The FSI technique was used to determine the force and the deformation of the blades by Yamaguchi and Okumura^[7]. After comparison, it was found that the analysis of a single blade did not match the actual situation. A periodic model was built to analyze the three-dimensional flow field and the unidirectional fluid solid coupling strength for various torque points of hydraulic torque converter. However, the outer ring and inner hub were not considered in the periodic model^[8,9]. Furthermore, the flow field of hydraulic torque converter under different working conditions was calculated and analyzed using the periodic symmetrical flow passage model. The result showed that the main reason for the deformation and fatigue failure of the blade was the fluid pressure^[10]. To sum up, the studies above made some feasible analysis and preliminary exploration about the FSI analysis in torque converters. However,

they had not taken the whole wheels into account to calculate the pressure, and the pressure loading may lead to the deformation and the fatigue of the torque converter^[7-10].

The rest of this paper is organized as follows. Firstly, FSI theory used in torque converters was deduced. Then, the model of the torque converter was built, and the fluid-solid interaction was calculated using ANSYS Workbench. Finally, the stress distribution was analyzed.

1 FSI theory in torque converters

In view of the small deformation of blades of torque converters, a one-way FSI method was used in this paper. The fluid pressure calculated by CFD (computational fluid dynamics) can be loaded to analyze the solid structure. The basic assumptions are as follows: (1) The transmission medium is incompressible. (2) The impeller blades are linear elastic bodies. (3) The disturbance of the structural distortion to the fluid field is ignored^[11-14].

1.1 N-S equations

The flow of fluid follows the rules^[15,16].

(1) Mass conservation equation:

① Supported by the Natural Science Foundation of Shaanxi Province of China (No. 2019JZ-10).

② To whom correspondence should be addressed. E-mail: huijz6363@chd.edu.cn

Received on Aug. 18, 2018

$$\frac{\partial \rho_f}{\partial t} + \nabla \cdot (\rho_f v) = 0 \quad (1)$$

the $\nabla \cdot v$ is 0 when the incompressible medium was assumed.

(2) Momentum conservation equation:

$$\frac{\partial v}{\partial t} \rho_f + \nabla \cdot (\rho_f v - \tau_f) = f_f \quad (2)$$

where t is time, f_f is the vector of body force, ρ_f is fluid density, v is the vector of fluid velocity, τ_f is shear stresses:

$$\tau_f = (-p + \mu \nabla \cdot v)I + 2\mu e \quad (3)$$

where p is fluid pressure, μ is dynamic viscosity, e is the tensor of speed stress:

$$e = \frac{1}{2}(\nabla v + \nabla v^T) \quad (4)$$

where ∇ is Hamilton operator: $\nabla = (\frac{\partial}{\partial x}, \frac{\partial}{\partial y}, \frac{\partial}{\partial z})$

1.2 Solid control equation

The solid conservation equation can be obtained by Newton's second law^[15,16]:

$$\rho_s \ddot{d}_s = \nabla \cdot \sigma_s + f_s \quad (5)$$

where ρ_s is the solid density, σ_s is the Cauchy tensor, f_s is the vector of volume, \ddot{d}_s is the vector of acceleration.

1.3 FSI equation

At the interface of FSI, solid stress (τ), displacement (d), heat flux (q), temperature (T) should be conserved^[15,16]:

$$\begin{cases} \tau_f n_f = \tau_s n_s \\ d_f = d_s \\ q_f = q_s \\ T_f = T_s \end{cases} \quad (6)$$

where subscript f refers to fluid, subscript s refers to solid.

1.4 FSI method of the torque converter

In order to obtain the distribution of stress and strain, FSI method was adopted^[17-19]. The fluid field was calculated by CFX, the pressure calculation of structure was carried out by ANSYS, and the FSI platform was applied by ANSYS-CFX.

As shown in Fig. 1, the process of FSI contains CFD and CSM (computational structural mechanics) modules. The CFD module was used to solve the N-S equations to obtain the fluid pressure load; while the CSM modules were used to solve the solid control equation to simulate the dynamic response. Both of them were

independent, and the interpolation was used to transfer the information by pressure value of the coupling surface^[17,20,21].

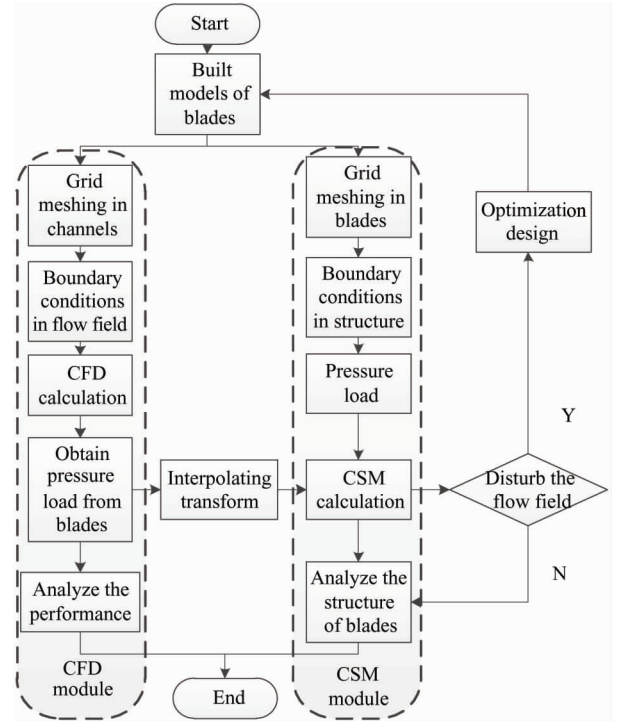


Fig. 1 FSI analysis process of hydrodynamic torque converter

2 FSI simulation of the torque converter

2.1 Model building

The point contour was scanned by the three-dimensional measuring instrument and the model was built by Pro/E and imported by ANSYS Design Modeler. As the wheels of the torque converter were rotational symmetry structure, the models can be divided into parts shown in Figs 2-4.

2.2 Model meshing

In order to simplify the simulation, ANSYS Meshing was used to divide the model into a periodic fluid channel instead of the whole torque converter. After comparing the meshing methods, the Hex Dominant Method was used to divide the structure into hexahedron, which could improve the accuracy and make it easier to converge. Since most components of torque converters were in thin-wall structure, it is appropriate to use the method of thin-solid swept^[17,20]. The grid divisions of the impeller, turbine and stator were shown in Figs 5-7.

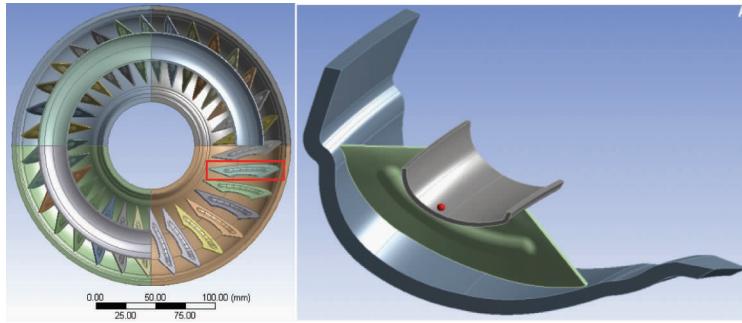


Fig. 2 Rotational symmetric structure of impeller

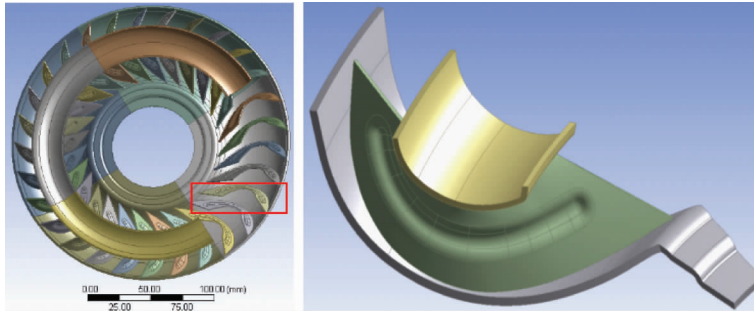


Fig. 3 Rotational symmetric structure of turbine

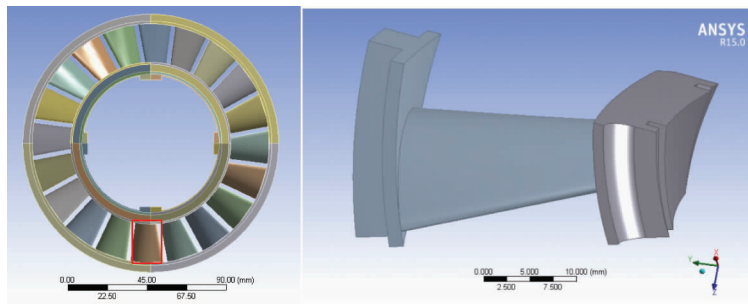


Fig. 4 Rotational symmetric structure of stator

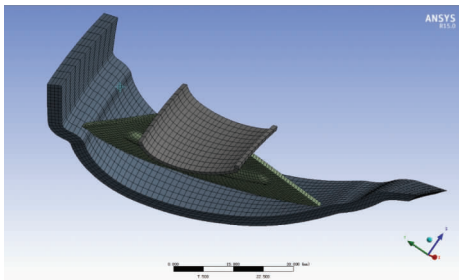


Fig. 5 Mesh of impeller

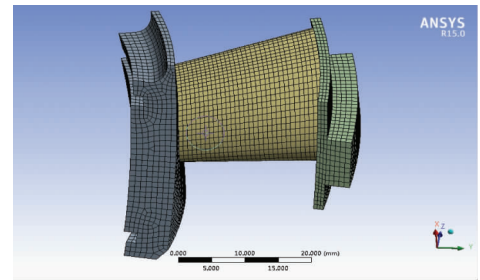


Fig. 7 Mesh of stator

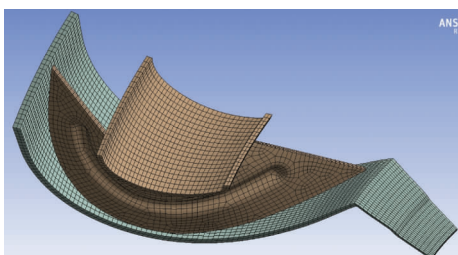


Fig. 6 Mesh of turbine

2.3 Numerical simulation

The whole fluid is an enclosed flow field in the CFD calculation. Hydraulic transmission oil was pumped in, which worked along with the wheels rotating around the shaft. Besides, the oil worked around the flow passage. The whole work completed the transformation between mechanical energy and hydraulic energy^[17,20,21]. Therefore, the surfaces were set as periodic boundaries, and the ring and hub were set as no-

slip boundary conditions.

Setting initial conditions are crucial for convergence of the calculation. Table 1 shows the key parameters of the torque converter. 8# hydraulic transmission oil was the working medium in the flow channel. Fluid pressure was mapped into the coupling surface (i. e. the fluid boundary), then the fluid pressure was calculated based on the model of the grid.

The rotating speed of the impeller was set as 2 000 rpm and the speed ratio was set as $i = 0, 0.1, 0.2, \dots, 0.8$, respectively. Usually, the torque converter can be locked-up (i. e. the impeller and the turbine are rigidly connected) when the speed ratio is more than 0.8.

Table 1 Parameters of the torque converter

	Impeller	Turbine	Stators
Blade number	31	29	20
Materials	SPCC	SPCC	ZL104
Density(kg/m^3)	7 850	7 850	2 650
Elasticity Modulus(Pa)	2.07×10^{11}	2.07×10^{11}	0.69×10^{11}
Poisson ratio	0.28	0.28	0.34

3 Results and discussion

In the simulation, the coupling surface of the blades was analyzed, and the pressure of the wheel structures was calculated.

The results showed that the stress distribution trend of each wheel was invariant at different working conditions, but the FSI effect was the most prominent at the low turbine speed and high impeller speed. So, the simulation conditions were set as $n = 2\ 000$ rpm, $i = 0$.

3.1 Analysis of blade pressure

Figs 8 – 10 show the imported pressure from the blades of impeller, turbine and stator.

(1) Pressure of the impeller blades

The impeller is connected with the engine as the entrance of power. Hydraulic transmission oil impacts the entrance of the impeller's blades when the impeller is actuated by the engine. The pressure is distributed equally along the flow channel. The maximum imported pressure is 0.16 MPa, appearing at the entrance of the impeller blades.

(2) Pressure of the turbine blades

The turbine wheel connects with the transmission shaft at the exit of the torque converter. The pressure of the blades are distributed evenly. The maximum im-

ported pressure is 0.136 MPa appearing at the exit of the turbine wheel's blades.

(3) Pressure of the stator blades

The stator is the key component of the torque converter and is used to improve the torque. The large pressure mainly concentrates on the surfaces between the entrance and the exit. The maximum imported pressure is 0.168 MPa.

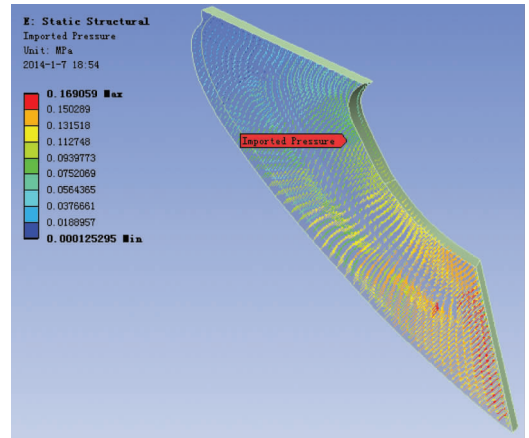


Fig. 8 Pressure from impeller blade

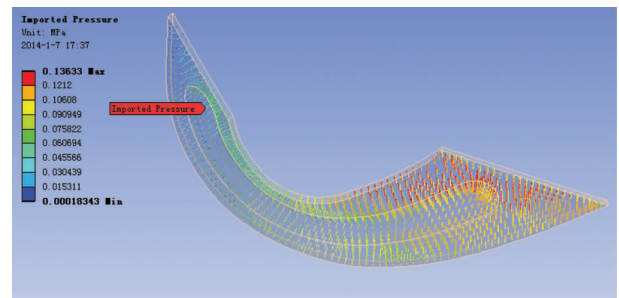


Fig. 9 Pressure from turbine blade

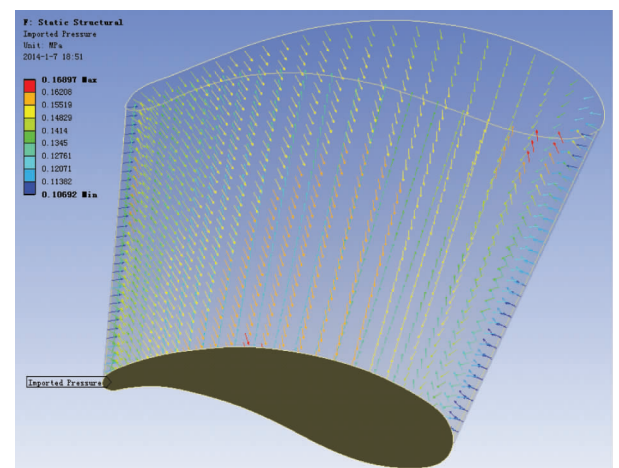


Fig. 10 Pressure from stator blade

3.2 Analysis of the wheels stress

The models of the blades are rotationally arranged due to the structure of the impeller, turbine and stator. Then the wheels are simulated, and the equivalent stress distributions can be shown in Figs 11 – 13.

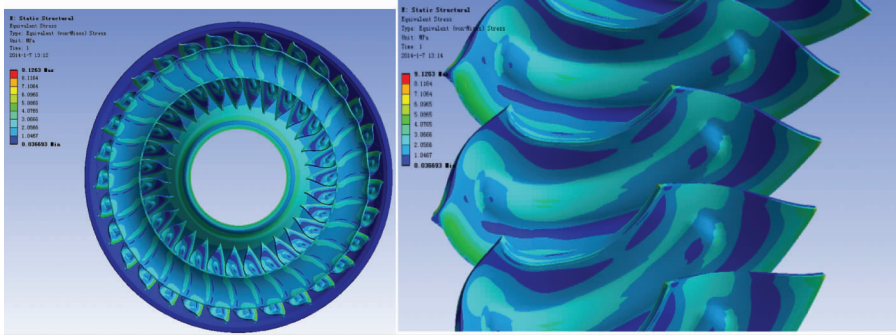


Fig. 11 Equivalent stress on impeller

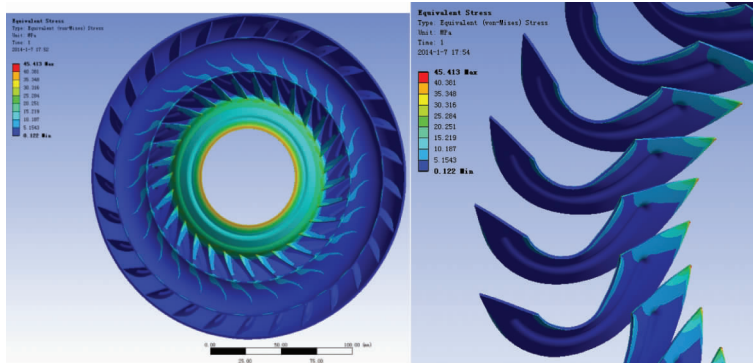


Fig. 12 Equivalent stress on turbine

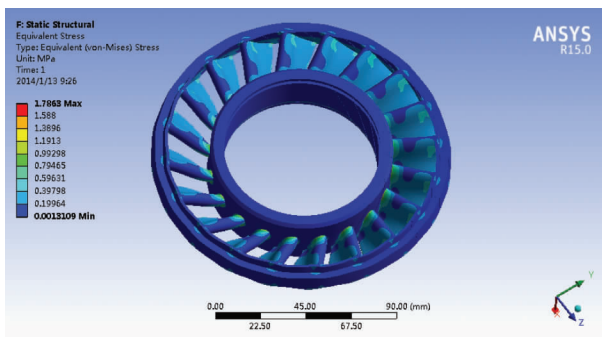


Fig. 13 Equivalent stress on stator 6

(2) Equivalent stress on the turbine

The turbine wheel's equivalent stress is much larger than the impeller's because the curvature of the turbine-wheel blades is larger than that of the impeller blades, and the blades and the shaft are rigidly connected. The maximum pressure is 45.4 MPa at the blades' corner near the shaft.

(3) Equivalent stress on the stator

The equivalent stress of the stator is not as much

(1) Equivalent stress on the impeller

The equivalent stress distribution of the impeller is mainly concentrated at the corner of the blades, especially at the junction of the hub and the blades. The maximum pressure of the impeller is 9.1 MPa.

as that of impeller wheel and the turbine wheel, because the blades are much thicker than the others. The stress concentrates mainly on the junctions, especially on the blades' corner. The maximum pressure is 1.78 MPa.

4 Conclusions

Compared with the traditional simulation, the FSI strength calculation of torque converters can reveal the pressure distribution of the wheels and blades. This paper provides a new method to calculate the pressure of torque converters. The results are summarized as follows:

(1) The maximum imported stress of the impeller blades is located at the entrance of the fluid, and the maximum equivalent stress of the impeller is located at the corner of the blades. The edge of the blades and the junction between the hub and the shell should be chamfered to reduce the pressure.

(2) The maximum imported stress of the turbine wheel blades is located at the exit of the fluid, and the maximum equivalent stress of the turbine wheel is located at the junction between the blades and the shaft. The length of the blades extending to the center of the shell should be shortened, the blades should be polished, and the chamfer should be sliced at the corner of the blades. Also, the junction between the turbine wheel and the shaft should be thickened.

(3) The stator is not easy to be damaged because it is thicker than the other wheels.

Reference

- [1] Keszy A, Kadziela A. Construction optimization of hydrodynamic torque converter with application of genetic algorithm[J]. *Archives of Civil and Mechanical Engineering*, 2001, 11:905-920
- [2] Hui J Z, Zheng H Y, Yang Y K, et al. Axial force calculation of sheet-metal-type hydraulic torque converter based on numerical solution of 3D flow field[J]. *China Journal of Highway and Transport*, 2016, 29: 145-152 (In Chinese)
- [3] Kotlinski J, Migus M, Keszy Z, et al. Fabrication of hydrodynamic torque converter impellers by using the selective laser sintering method[J]. *Rapid Prototyping Journal*, 2013, 19(6):430-436
- [4] Keszy A. Mathematical model of a hydrodynamic torque converter for vehicle power transmission system optimisation[J]. *International Journal of Vehicle Design*, 2012, 59(1):1-22
- [5] Jung J H, Kang S, Hur N. A numerical study of a torque converter with various methods for the accuracy improvement of performance prediction[J]. *Progress in Computational Fluid Dynamics An International Journal*, 2011, 11(3-4):261-268
- [6] Atallah A M, Tantawy E S F E. Direct torque control of machine side multilevel converter for variable speed wind turbines[J]. *Energy*, 2015, 90:1091-1099
- [7] Yamaguchi T, Okumura A. Torque converter stress analysis by transient FSI technique [C]. In: ASME-JSME-KSME 2011 Joint Fluids Engineering Conference, Hamamatsu, Japan, 2011. 2205-2210
- [8] Liu C, Pan X, Yan Q D, et al. Effect of blade number on performance of torque converter and its optimization based on doe and response surface methodology [J]. *Transactions of Beijing Institute of Technology*, 2012, 32: 689-693
- [9] Liu S , Xing Q K, Li W W, et al. A mixed flow channel CFD simulation method for vehicle torque converter[J]. *China Mechanical Engineering*, 2016, 27(7):989-993
- [10] Wu G, Wang L. Application of dual-blade stator to low-speed ratio performance improvement of torque converters [J]. *Chinese Journal of Mechanical Engineering*, 2016, 29(2):293-300
- [11] Cilla M, Borrás I, Peña E, et al. A parametric model for analysing atherosclerotic arteries: on the FSI coupling [J]. *International Communications in Heat & Mass Transfer*, 2015, 67:29-38
- [12] Tian F B, Wang Y, John Young, et al. An FSI solution technique based on the DSD/SST method and its applications[J]. *Mathematical Models & Methods in Applied Sciences*, 2015, 25(12):2257-2285
- [13] Roshchenko A, Mineev P D, Finlay W H. A time splitting fictitious domain algorithm for fluid-structure interaction problems (A fictitious domain algorithm for FSI) [J]. *Journal of Fluids & Structures*, 2015, 58:109-126
- [14] Baaijens F P T. A fictitious domain/mortar element method for fluid-structure interaction [J]. *International Journal for Numerical Methods in Fluids*, 2015, 35(7):743-761
- [15] Bungartz H J, Schäfer M. Fluid-structure interaction: modelling, simulation, optimisation [J]. *Lecture Notes in Computational Science & Engineering*, 2006, 53:233-269
- [16] Ozdemir Z, Souli M, Fahjan Y M. Application of nonlinear fluid-structure interaction methods to seismic analysis of anchored and unanchored tanks [J]. *Engineering Structures*, 2010, 32(2):409-423
- [17] Boffi D, Cavallini N, Gastaldi L. Finite element approach to immersed boundary method with different fluid and solid densities [J]. *Mathematical Models & Methods in Applied Sciences*, 2011, 21(12):2523-2550
- [18] Burman E, Fernández M A. An unfitted Nitsche method for incompressible fluid-structure interaction using overlapping meshes [J]. *Computer Methods in Applied Mechanics & Engineering*, 2014, 279(1):497-514
- [19] Degroote J, Vierendeels J. Multi-level quasi-Newton coupling algorithms for the partitioned simulation of fluid-structure interaction [J]. *Computer Methods in Applied Mechanics & Engineering*, 2012, 225-228(2):14-27
- [20] Gee M W, Küttler U, Wall W A. Truly monolithic algebraic multigrid for fluid-structure interaction [J]. *International Journal for Numerical Methods in Engineering*, 2011, 85(8):987-1016
- [21] Massing A, Larson M G, Logg A. Efficient implementation of finite element methods on non-matching and overlapping meshes in 3D [J]. *SIAM Journal on Scientific Computing*, 2013, 35(1):C23-C47

Zhang Zeyu, born in 1990. He received his Ph. D degree in Mechanical Electronic Engineering Department of Chang'an University in 2018. He received his M. S. degree from Chang'an University in 2015 and received his B. S. degree from Shanghai University of Engineering Science respectively. His research interests include the integration of mechatronics hydraulics, the transmission of construction machinery and machine learning.